JPE 19-5-4

https://doi.org/10.6113/JPE.2019.19.5.1099
ISSN(Print): 1598-2092 / ISSN(Online): 2093-4718

Analysis of Hybrid Converter with Wide Voltage Range Operation

Bor-Ren Lin†

†Department of Electrical Engineering, National Yunlin University of Science and Technology, Yunlin, Taiwan

Abstract

A soft switching converter with wide voltage range operation is investigated in this paper. A series resonant converter is implemented to achieve a high circuit efficiency with soft switching characteristics on power switches and rectifier diodes. To improve the weakness of the narrow voltage range in LLC converters, an alternating current (ac) power switch is used on the primary side to select a half-bridge or full-bridge resonant circuit to implement 4:1 voltage range operation. On the secondary-side, another ac power switch is adopted to select a full-wave rectifier or voltage-doubler rectifier to achiever an additional 2:1 output voltage range. Therefore, the proposed resonant converter has the capacity for 8:1 (320V~40V) wide output voltage operation. A single-stage hybrid resonant converter is employed in the study circuit instead of a two-stage dc converter to achiever wide voltage range operation. As a result, the study converter has better converter efficiency. The theoretical analysis and circuit characteristics are verified by experiments with a prototype circuit.

Key words: Hybrid resonant circuit, Soft switching operation, Wide voltage operation

I. INTRODUCTION

High power density and high efficiency power converters with wide voltage range operations [1]-[5] have been presented and investigated for the power units in railway vehicles, battery chargers in electric vehicles and outdoor LED lighting systems. On railway system applications, the input voltages of dc converters are from 24V to 110V for the lighting, electric door system, motor drive controller and braking system demands. To meet international standard such as EN50155, the input voltage variation of dc converters must be within ±30% or ±40% of its nominal voltage. For the battery chargers in electric vehicles, the output voltage of dc converters are from 200V to 450V. Dc converters with a variable output voltage and a constant power rating are needed for outdoor LED lighting systems. Therefore, soft switching converters with wide voltage range operation are needed for solar power units, electric vehicles, high speed rail vehicles and outdoor LED lighting systems. Conventional two-stage dc-dc converters [6]-[8] have been used to realize wide voltage operation. The front-stage circuit topologies can be buck, buck-boost or boost circuit topologies and the rear-stage circuits can be full-bridge, half-bridge or push-pull circuits. However, the efficiency of two-stage converters is lower than that of single-stage circuits. Dc-dc converters with series or parallel connections were presented in [9]-[11] to achieve wide input or output voltage range operations. The disadvantage of these topologies is the large number of circuit components, which decreases the efficiency and reliability. Full/half bridge dc-dc circuits with phase-shift control and a wide input/output voltage range were presented in [12] and [13]. However, their control strategy is too complicated to be implemented with general integrated circuits. Resonant circuits have been developed in [14]-[17] to accomplish wide voltage operation. However, the operating voltage range is limited at 4:1, i.e., $V_{in,max}$=4$V_{in,min}$ (or $V_{o,max}$=4$V_{o,min}$). Dc converters with much wider voltage range operation are normally welcome for railway vehicle power units, solar power conversion and output LED lighting power units.

A hybrid converter with wide output voltage range operation (8:1 output voltage range, 320V~40V) and zero voltage switching is presented and investigated. Full-bridge or half-bridge resonant circuits can be selected on the primary side using an alternating current (ac) power switch to achieve zero-voltage switching characteristic for all of the active

Manuscript received Mar. 8, 2019; accepted May 14, 2019
Recommended for publication by Associate Editor Jongwon Shin.
†Corresponding Author: linbr@yuntech.edu.tw
Tel: +886-912312281, Fax: +886-5-5312065
Dept. of Electrical Eng., Nat'l Univ. of Science and Technology, Taiwan

© 2019 KIPE

devices. Since the fundamental primary-side voltage of a full-bridge circuit is two times the fundamental voltage of a half-bridge circuit, the proposed converter can achieve 4:1 voltage range operation on the input side. A half-bridge voltage-doubler rectifier or a full-bridge diode rectifier can be selected on output side using an auxiliary ac power switch to achieve another 2:1 voltage range operation. Therefore, an 8:1 wide voltage range operation is accomplished in the developed circuit. When compared to conventional two-stage converters or the other wide voltage range converters, the circuit topology and control strategy of the presented hybrid resonant circuit are easy to implement. The theoretical analysis, operation principle and circuit characteristics are investigated and confirmed by experiments based on a laboratory prototype.

II. CIRCUIT STRUCTURE

The circuit configuration of the proposed wide voltage range resonant circuit is provided in Fig. 1. S_1-S_4 are power MOSFETs. Q_1 and Q_2 are ac power switches implemented by two power MOSFETs with a back-to-back connection. C_r is the resonant capacitor. C_1 and C_2 are the input split capacitors. C_{o1} and C_{o2} are the output split capacitors. L_r is the resonant inductor. T is the isolation transformer. L_m is the magnetizing inductance of T. D_1-D_4 are the rectifier diodes. D_{S1}-D_{S4} are the body diodes, and C_{S1}-C_{S4} are the output capacitances of S_1-S_4. V_{in} and V_o are the input and output voltages, and R_o is the output resistor. L_m, L_r and C_r are worked as the *LLC* resonant tank to realize the advantages of soft switching turn-on characteristic for S_1-S_4 and turn-off characteristic for D_1-D_4. Therefore, the switching loss and electromagnetic interference of the proposed converter are decreased and improved. To implement wide voltage operation, two ac switches Q_1 and Q_2 are used on the primary and secondary sides, respectively. Owing to the on/off states of Q_1 and Q_2, three output voltage ranges ($V_{o,min}$~$2V_{o,min}$, $2V_{o,min}$~$4V_{o,min}$ and $4V_{o,min}$~$8V_{o,min}$) are achieved. Fig. 2(a) gives the operating circuit when V_o is on the low voltage range ($V_{o,min}$~$2V_{o,min}$). For the low voltage range, Q_1 is on and Q_2 is off. The input side is a half-bridge resonant converter and the output side is a full-bridge diode rectifier. The voltage gain on this equivalent circuit is low when compared to the other two operation ranges. The operating circuit for the medium output voltage range ($2V_{o,min}$~$4V_{o,min}$) is provided in Fig. 2(b). Q_1 and Q_2 are both on. The input side is a half-bridge resonant converter and the output side is a half-bridge voltage-doubler rectifier. The voltage gain of this equivalent circuit (Fig. 2(b)) is two times of the gain of the low voltage range operation shown in Fig. 2(a). An equivalent circuit for high voltage range operation is shown in Fig. 2(c). Q_1 is off and Q_2 is on. The input side is a full-bridge resonant converter and the output side is a voltage-doubler rectifier. The voltage gain of this equivalent circuit (Fig. 2(c)) is two times the gain for medium voltage range operation (Fig. 2(b)).

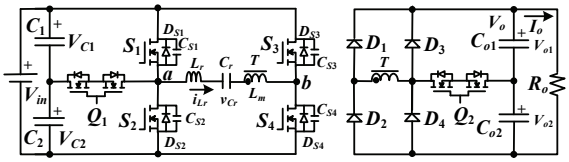

Fig. 1. Circuit diagram of the proposed converter with wide voltage range operation.

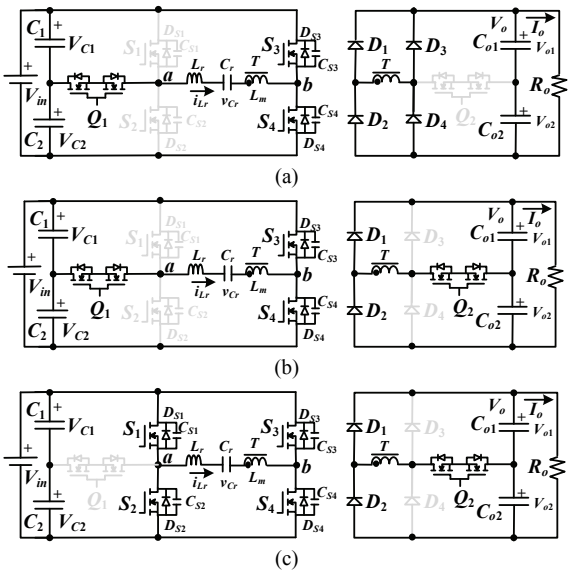

Fig. 2. Equivalent circuits for different output voltage ranges. (a) Low voltage output. (b) Medium voltage output. (c) High voltage output.

From the on and off conditions of Q_1 and Q_2 and the PWM signals of S_1-S_4, the resonant converter with wide voltage range operation is implement in the proposed converter.

III. OPERATION PRINCIPLE

Two ac power switches Q_1 and Q_2 are controlled for different output voltage ranges. According to the on/off states of Q_1 and Q_2, the proposed converter has three output voltage operation ranges $V_{o,min}$~$2V_{o,min}$, $2V_{o,min}$~$4V_{o,min}$ and $4V_{o,min}$~$8V_{o,min}$. Theoretical circuit waveforms and equivalent circuits for the three output voltage ranges are provided in Figs. 3~5.

A. Low Output Voltage Range (Q1 on; S1, S2, Q2 off)

To provide a low voltage output (Fig. 2(a)), Q_1 is turned on, and S_1, S_2 and Q_2 are turned off for low voltage output operation. The input side is a half-bridge resonant converter. The output side is a full-wave diode rectifier. The voltage gain at low voltage output operation is $G_L=2nV_{o,L}/V_{in}$, where n is the turn-ratio of T, and $V_{o,L}$ is the load voltage under the low output voltage range. Fig. 3 shows theoretical circuit waveforms and equivalent circuits for six operating modes.

Mode 1 [t_0, t_1]: $v_{CS4}=0$ at t_0. Owing to $i_{Lr}(t_0)<0$, D_{S4} is forward biased, and S_4 is turned on at zero-voltage switching. C_r and L_r are naturally resonant. In mode 1, D_1 and D_4 conduct

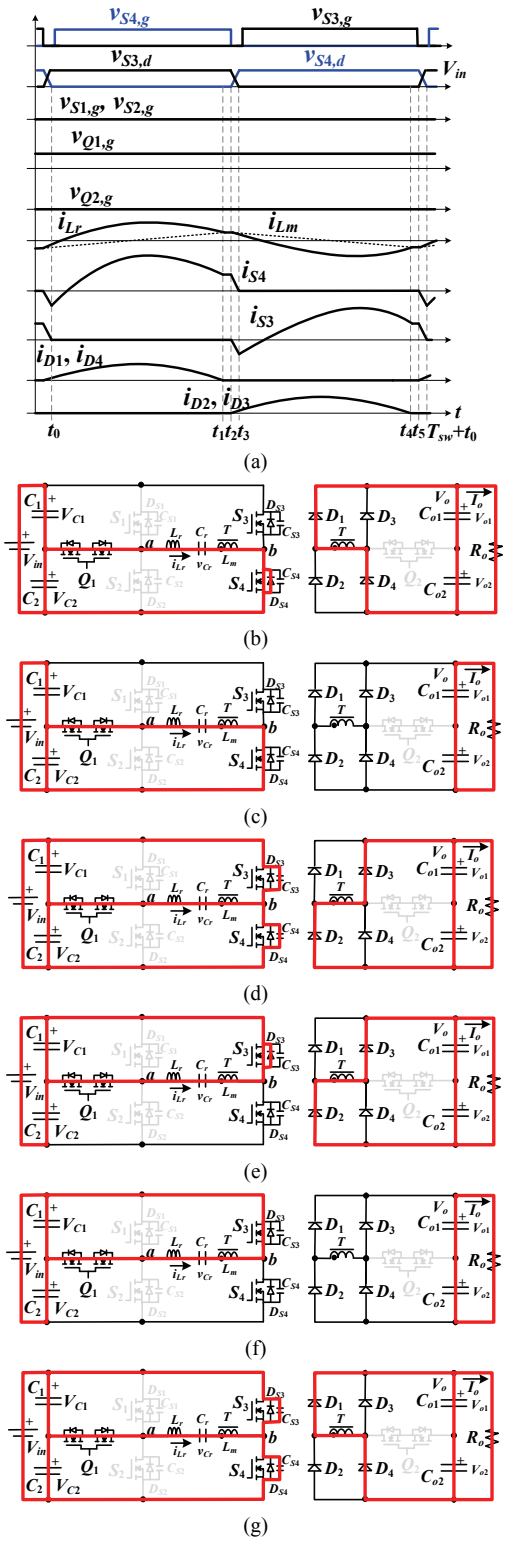

Fig. 3. Proposed converter for the low output voltage range. (a) Pulse-width modulation waveforms. (b) Mode 1. (c) Mode 2. (d) Mode 3. (e) Mode 4. (f) Mode 5. (g) Mode 6.

so that $v_{Lm}=nV_o$, i_{Lm} increases, and C_{o1} and C_{o2} are charged.

Mode 2 [t_1, t_2]: If the series resonant frequency f_r is greater than the switching frequency, i_{Lr} is equal to i_{Lm} at t_1. Therefore, D_1 and D_4 are turned off. The components L_m, C_r and L_r are naturally resonant.

Mode 3 [t_2, t_3]: S_4 is turned off at t_2. Because of $i_{Lr}(t_2)>0$, C_{S3} (C_{S4}) is discharged (charged). Since $i_{Lm}(t_2)> i_{Lr}(t_2)$, D_2 and D_3 are forward biased, and $v_{Lm}=-nV_o$. The capacitances of C_{S3} and C_{S4} are about hundreds of a picofarad (pF). Thus, the discharge and charge times in this mode are fast enough, and the current values are almost constant.

Mode 4 [t_3, t_4]: $v_{CS3}=0$ at t_3. Because of $i_{Lr}(t_3)>0$, D_{S3} is forward biased, and S_3 is turned on under zero voltage. In mode 4, D_2 and D_3 are conducting, $v_{Lm}=-nV_o$, and C_r and L_r are naturally resonant.

Mode 5 [t_4, t_5]: If $f_r > f_{sw}$, the primary current i_{Lr} is equal to i_{Lm} at t_4, and D_1-D_4 are off. In this mode, L_m, L_r and C_r are naturally resonant.

Mode 6 [t_5, $T_{sw}+t_0$]: S_3 is turned off at t_5. Due to $i_{Lr}(t_5)<0$ and $i_{Lm}(t_5)<i_{Lr}(t_5)$, C_{S3} (C_{S4}) is charged (discharged), and D_1 and D_4 conduct. At $T_{sw}+t_0$, $v_{CS4}=0$. Then, the converter goes to next operating cycle.

B. Medium Output Voltage Range (Q1, Q2 on; S1, S2, D3, D4 off)

Fig. 2(b) provides an equivalent circuit for the medium voltage output. For the medium output voltage range, Q_1 and Q_2 are on, and S_1, S_2, D_3 and D_4 are off. The circuit topology includes a half-bridge converter on the input side and a half-wave voltage-doubler rectifier on the output side. The dc voltage gain of the proposed converter operating at the medium output voltage range is $G_M=nV_{o,M}/V_{in}$, where $V_{o,M}$ is the load voltage for medium voltage output operation. Comparing the low and medium output voltage range operations, it can observe that $V_{o,M}=2V_{o,L}$ under the same input voltage V_{in} and dc voltage gains $G_L=G_M$. Fig. 4 provides theoretical circuit waveforms and equivalent circuits for six operating modes at the medium output voltage operation.

Mode 1 [t_0, t_1]: $v_{CS4}=0$ at t_0. Because of $i_{Lr}(t_0)<0$, D_{S4} conducts, and S_4 is turned on under zero voltage. Due to $i_{Lr} > i_{Lm}$, D_1 conducts, C_{o1} is charged by i_{D1}, and C_{o2} is discharged to supply the load current. In mode 1, $v_{Lm}=nV_{o1}=nV_o/2$, and L_r and C_r are naturally resonant.

Mode 2 [t_1, t_2]: At t_1, $i_{Lr}=i_{Lm}$. Thus, D_1 is off, and C_{o1} and C_{o2} are both discharged to supply the load power. On the primary side, L_m, C_r and L_r are naturally resonant.

Mode 3 [t_2, t_3]: S_4 is turned off at t_2. Due to $i_{Lr}(t_2)>0$ and $i_{Lm}(t_2)>i_{Lr}(t_2)$, C_{S3} (C_{S4}) is discharged (charged), and D_2 conducts. C_{o1} is discharged, and C_{o2} is charged by i_{D2}.

Mode 4 [t_3, t_4]: $v_{CS3}=0$ at t_3. Since $i_{Lr}(t_3)>0$, D_{S3} conducts, and S_3 is turned on under zero voltage. On the secondary side, D_2 conducts, $v_{Lm}=-nV_{o2}=-nV_o/2$ and C_{o2} is charged. C_r and L_r are naturally resonant in this mode.

Mode 5 [t_4, t_5]: At t_4, $i_{Lr}=i_{Lm}$. Thus, D_2 is reverse biased, and C_{o1} and C_{o2} are discharged. L_m, L_r and C_r are naturally resonant.

Mode 6 [t_5, $T_{sw}+t_0$]: S_3 is turned off at t_5. Because $i_{Lr}>i_{Lm}$

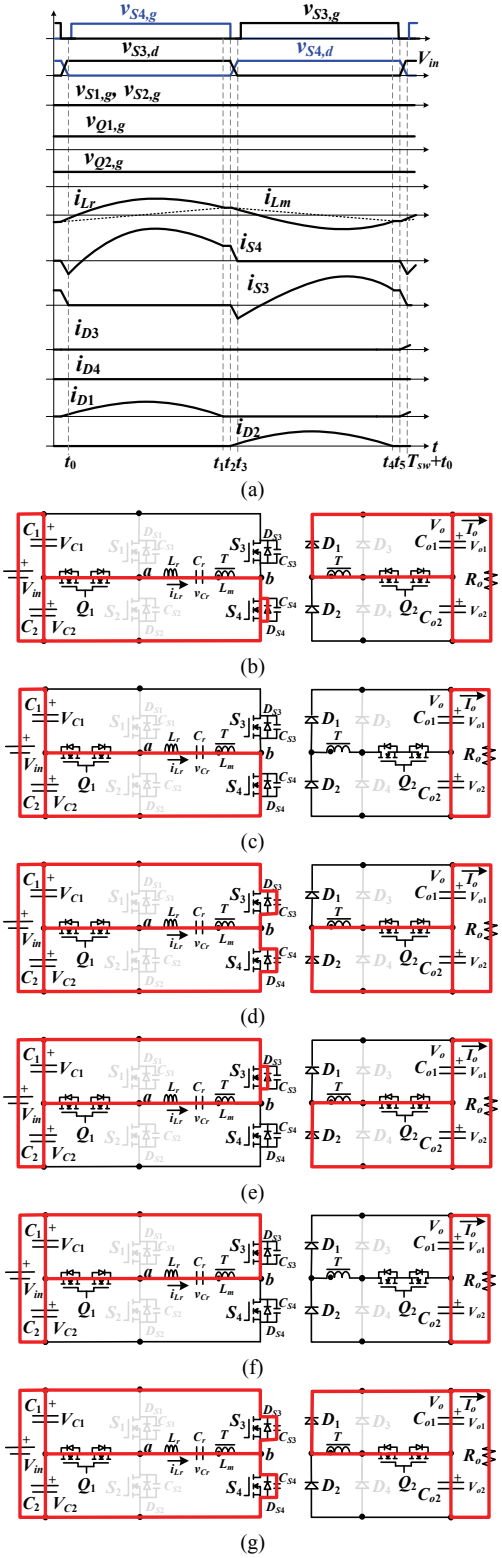

Fig. 4. Proposed converter for the medium output voltage range. (a) Pulse-width modulation waveforms. (b) Mode 1. (c) Mode 2. (d) Mode 3. (e) Mode 4. (f) Mode 5. (g) Mode 6.

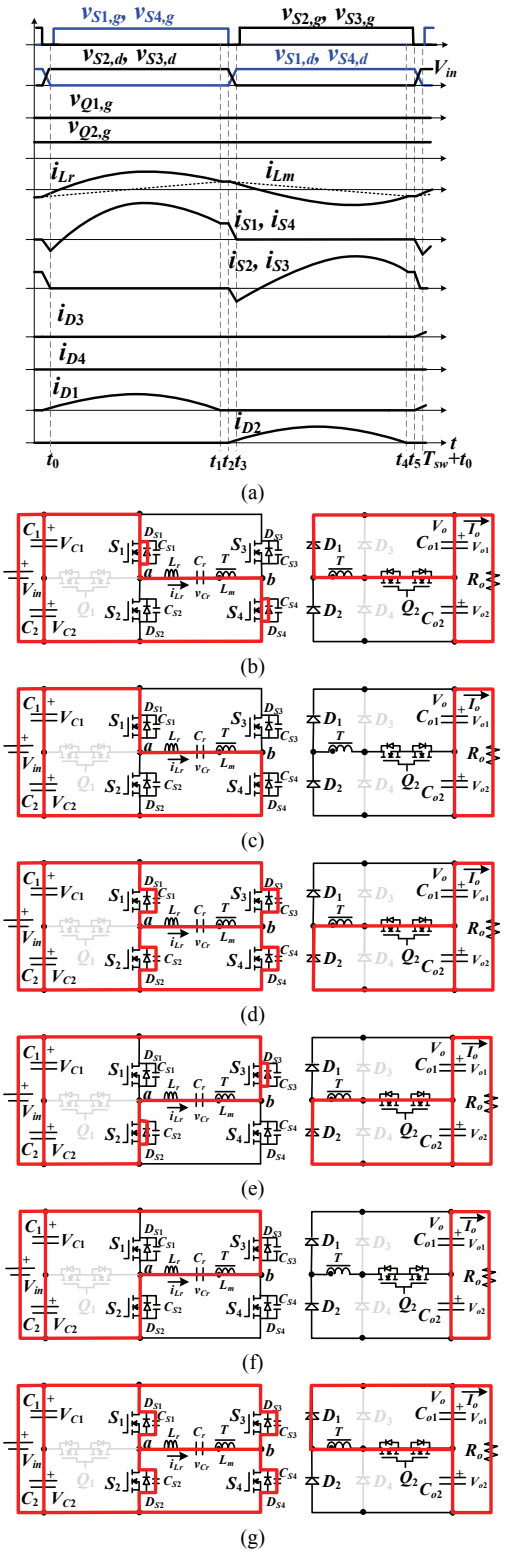

Fig. 5. Proposed converter for the high output voltage range. (a) Pulse-width modulation waveforms. (b) Mode 1. (c) Mode 2. (d) Mode 3. (e) Mode 4. (f) Mode 5. (g) Mode 6.

and $i_{Lr}(t_5)<0$, D_1 conducts, and C_{S3} (C_{S4}) is charged (discharged). At $T_{sw}+t_0$, $v_{CS4}=0$. Then, the converter goes to next operating cycle.

C. High Output Voltage Range (Q2 on; Q1, D3, D4 off)

An equivalent circuit for high output voltage range operation is given in Fig. 2(c). Q_2 is turned on, and Q_1, D_3

and D_4 are in the off-state. The input side is a full-bridge resonant circuit and the output side is a half-wave voltage-doubler rectifier. The dc voltage gain for high voltage range operation is $G_H=nV_{o,H}/(2V_{in})$, where $V_{o,H}$ is the load voltage at high voltage output operation. Comparing G_L, G_M and G_H, it is possible to obtain $V_{o,H}=2V_{o,M}=4V_{o,L}$ under the same dc voltage gains $G_L=G_M=G_H$. Fig. 5 shows theoretical circuit waveforms and equivalent circuits for six operating modes at high output voltage operation.

Mode 1 [t_0, t_1]: $v_{CS4}=0$ at t_0. Since $i_{Lr}(t_0)<0$, D_{S1} and D_{S4} conduct. Therefore, S_1 and S_4 turn on under zero-voltage switching. D_1 conducts, and C_{o1} is charged. In this mode, $v_{Lm}=nV_o/2$, and C_r and L_r are naturally resonant.

Mode 2 [t_1, t_2]: The primary current i_{Lr} is decreased and equal to i_{Lm} at t_1. Then, the diode D_1 becomes reverse biased. In this mode, both C_{o1} and C_{o2} are discharged, and L_m, L_r and C_r are naturally resonant.

Mode 3 [t_2, t_3]: S_1 and S_4 are turned off at t_2. Due to $i_{Lr}(t_2)>0$ and $i_{Lm}(t_2)>i_{Lr}(t_2)$, C_{S2} and C_{S3} discharge. Diode D_2 conducts, and C_{o2} is charged.

Mode 4 [t_3, t_4]: At time t_3, $v_{CS2}=v_{CS3}=0$. Due to $i_{Lr}(t_3)>0$, D_{S2} and D_{S3} are forward biased, and S_2 and S_3 are turned on at zero-voltage switching. In this mode, D_2 conducts, C_{o2} is charged, $v_{Lm}=-nV_o/2$, and C_r and L_r are naturally resonant.

Mode 5 [t_4, t_5]: The primary current i_{Lr} is equal i_{Lm} at t_4. Then, D_2 becomes reverse biased. Both C_{o1} and C_{o2} are discharged. L_m, L_r and C_r are naturally resonant.

Mode 6 [t_5, $T_{sw}+t_0$]: At time t_5, the MOSFETs S_2 and S_3 are turned off. Due to $i_{Lr}(t_5)>i_{Lm}(t_5)$ and $i_{Lr}(t_5)<0$, D_1 becomes forward biased, and C_{S1} and C_{S4} are discharged. At $T_{sw}+t_0$, $v_{CS1}=v_{CS4}=0$. Then, the circuit goes to next operating cycle.

IV. Circuit Analysis

Three voltage ranges can be operated in the proposed circuit by selection the half-bridge or full-bridge resonant circuit on input side and the full-wave rectifier or half-bridge voltage-doubler rectifier on the output side. Since an *LLC* series resonant circuit is employed on the input side to achieve soft switching operation for both the switches and passive diodes, variable frequency modulation is used to regulate the output voltage. The fundamental harmonic frequency method is selected to analyze and estimate the voltage gains of the resonant tank for three output voltage ranges according to the on/off states of Q_1 and Q_2. When Q_1 is in the on-state under low and medium voltage ranges, a square voltage waveform with voltage values of $\pm V_{in}/2$ is generated on the voltage v_{ab}. If the proposed converter is operated at high voltage range operation, Q_1 is off and a square voltage waveform with voltage values of $\pm V_{in}$ is shown on the voltage v_{ab}. Therefore, the fundamental value of the root-mean-square (*rms*) voltage $V_{ab,rms}$ is determined by:

$$V_{ab,rms}=\begin{cases}\sqrt{2}V_{in}/\pi, & Q_1 \text{ on}\\ 2\sqrt{2}V_{in}/\pi, & Q_1 \text{ off}\end{cases} \tag{1}$$

In the same way, the fundamental *rms* value of the magnetizing voltage $V_{Lm,rms}$ is determined by:

$$V_{Lm,rms}=\begin{cases}\sqrt{2}nV_o/\pi, & Q_2 \text{ on}\\ 2\sqrt{2}nV_o/\pi, & Q_2 \text{ off}\end{cases} \tag{2}$$

Based on the dc output resistor, the ac equivalent resistor is determined by:

$$R_{ac}=\begin{cases}\dfrac{2n^2R_o}{\pi^2}, & Q_2 \text{ on}\\ \dfrac{8n^2R_o}{\pi^2}, & Q_2 \text{ off}\end{cases} \tag{3}$$

Therefore, the resonant tank consists of the *rms* voltage $V_{ab,rms}$, L_r, C_r, L_m and R_{ac}. The ac voltage gain of resonant tank is obtained as:

$$|G|=\frac{V_{Lm,rms}}{V_{ab,rms}}=\frac{1}{\sqrt{[1+\frac{1}{L_n}\frac{F^2-1}{F^2}]^2+X^2(\frac{F^2-1}{F})^2}}$$
$$=\begin{cases}\dfrac{2nV_{o,L}}{V_{in}}, & Q_1 \text{ on } \& \ Q_2 \text{ off}\\ \dfrac{nV_{o,M}}{V_{in}}, & Q_1 \text{ on } \& \ Q_2 \text{ on}\\ \dfrac{nV_{o,H}}{2V_{in}}, & Q_1 \text{ off } \& \ Q_2 \text{ on}\end{cases} \tag{4}$$

where $F=f_s/f_r$ is the frequency ratio, $L_n=L_m/L_r$ is the inductor ratio, and $X=\sqrt{L_r/C_r}/R_{ac}$ is quality factor. From (4), the output voltage at different voltage ranges is expressed as:

$$V_{o,H}=\frac{2V_{in}}{n\sqrt{[1+\frac{1}{L_n}\frac{F^2-1}{F^2}]^2+X^2(\frac{F^2-1}{F})^2}} \tag{5}$$

$$V_{o,M}=\frac{V_{in}}{n\sqrt{[1+\frac{1}{L_n}\frac{F^2-1}{F^2}]^2+X^2(\frac{F^2-1}{F})^2}} \tag{6}$$

$$V_{o,L}=\frac{V_{in}}{2n\sqrt{[1+\frac{1}{L_n}\frac{F^2-1}{F^2}]^2+X^2(\frac{F^2-1}{F})^2}} \tag{7}$$

According to the output voltage demand, Q_1 and Q_2 are controlled to have wide output voltage capability. Since the operating frequency is greater than the series resonant frequency under all of the load conditions and input and output voltage values, the input impedance at the resonant tank is always operated at the inductive impedance. Therefore, the power MOSFETs S_1-S_4 can be operated under soft switching turn-on.

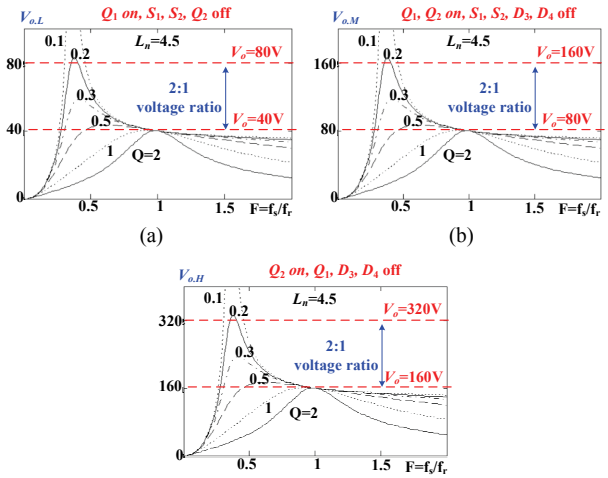

Fig. 6. Output voltage due to different voltage ranges. (a) Low voltage output. (b) Medium voltage output. (c) High voltage output.

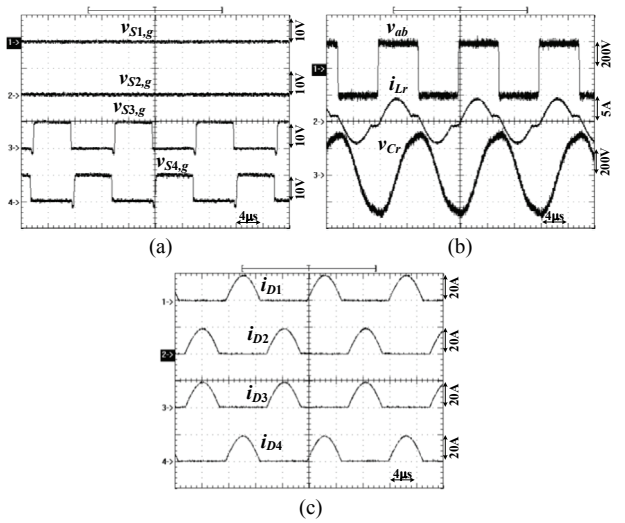

Fig. 7. Measured results at V_o=40V in the low output voltage range. (a) Gating signals $v_{S1,g}$ ~ $v_{S4,g}$ at a full load. (b) Primary side voltages and current v_{ab}, i_{Lr} and v_{Cr} at a full load. (c) Diode currents i_{D1} ~ i_{D4} at a full load.

V. Design Procedure and Experimental Results

To investigate the effectiveness of the proposed circuit, a laboratory prototype was assembled and experimented on with a constant input voltage V_{in}=400V which is generated by a power factor correction circuit. The output voltage V_o can be changed from 40V to 320V (8:1 ratio). The design resonant frequency f_r is 100kHz. The rated load power $P_{o,max}$ is 400W. Based on the fundamental ac voltage gain in (4), output voltage curves for the three output voltage ranges are provided in Fig. 6 under a 400V input. From (4), it can observe that the ac voltage gains of the resonant tank under the three voltage ranges are identical. In each voltage range, the minimum voltage gain G_{min} in (4) is designed at unity, and the maximum voltage gain G_{max} is intended at two. Thus, the resonant tank in each voltage range can achieve 2:1 voltage ratio operation, and 8:1 wide voltage ratio operation can be achieved in the proposed converter. To accomplish this function, a low inductor ratio L_n=4.5 and a low quality factor are used. There is a ±2V voltage tolerance in the transient voltages such as 80V (160V) between the low (medium) voltage range and the medium (high) voltage range. Under the low output voltage range, Q_1 is on and S_1, S_2 and Q_2 are off. The input side has a half-bridge resonant circuit, and the output side has a full-wave rectifier. The maximum and minimum output voltages are 80V and 40V, respectively. The designed voltage gains at the maximum and minimum output voltages are two and unity, respectively. The turn-ratio n can be calculated in (8).

$$n=\frac{G_{L,\min}V_{in}}{2V_{o,L,\min}}=\frac{1\times 400}{2\times 40}=5 \tag{8}$$

A TDK ferrite core EER-42 is used for the transformer T, with n_p=60 turns and n_s=12 turns. Under the rated power and V_o=80V conditions, the fundamental equivalent resistance on the primary side approximates:

$$R_{ac}=\frac{8n^2R_o}{\pi^2}=\frac{8\times 5^2\times(80^2/400)}{3.14159^2}\approx 324\Omega \tag{9}$$

Based on the given parameters, X=0.2, L_n=4.5 and f_r=100kHz, L_r, L_m and C_r are determined in (10)~(12).

$$L_r=\frac{XR_{ac}}{2\pi f_r}=\frac{0.2\times 324}{2\pi\times 100000}\approx 103\,\mu\text{H} \tag{10}$$

$$L_m=L_rL_n=103\times 4.5=463.5\,\mu\text{H} \tag{11}$$

$$C_r=\frac{1}{4\pi^2L_rf_r^2}=\frac{1}{4\pi^2\times 103\times 10^{-6}\times(100000)^2}\approx 24.6\text{nF} \tag{12}$$

In the prototype, the selected resonant components are L_r=100μH, L_m=450μH and C_r=25nF. The voltage stresses of the power switches and diodes can be approximately calculated as.

$$V_{S1,stress}=..=V_{S4,stress}=V_{in}=400\,\text{V} \tag{13}$$

$$V_{Q1,stress}=V_{in}/2=200\text{V} \tag{14}$$

$$V_{Q2,stress}=V_{o,L,\max}/2=40\text{V} \tag{15}$$

$$V_{D1,stress}=V_{D2,stress}=V_{o,\max}=320V \tag{16}$$

$$V_{D3,stress}=V_{D4,stress}=V_{o,\max}/2=160V \tag{17}$$

MOSFETs 48N60DM2 (600V40A) are adopted for Q_1 and Q_2, 22NM60N (650V16A) are used for S_1~S_5, and STTH12R06D (600V12A) are adopted for D_1~D_4. The selected capacitances are C_1=C_2=300μF/400V and C_{o1}=C_{o2}= 1350μF/400V.

The maximum power of the prototype is 400W. The three output voltage ranges can be controlled in the adopted control

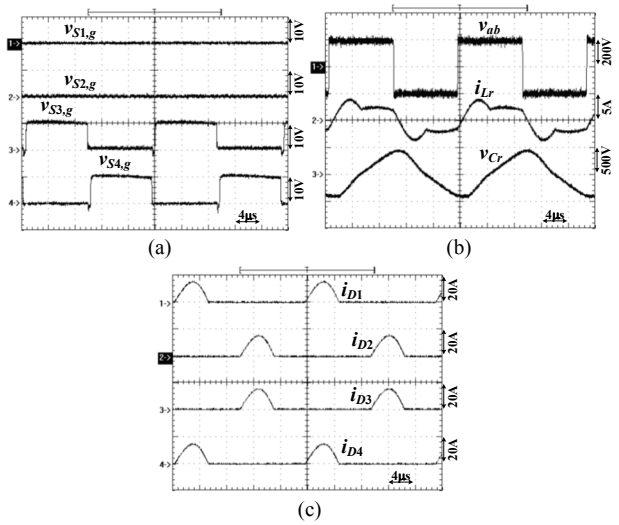

Fig. 8. Measured results at V_o=78V in the low output voltage range. (a) Gating signals $v_{S1,g} \sim v_{S4,g}$ at a full load. (b) Primary side voltages and current v_{ab}, i_{Lr} and v_{Cr} at a full load. (c) Diode currents $i_{D1} \sim i_{D4}$ at a full load.

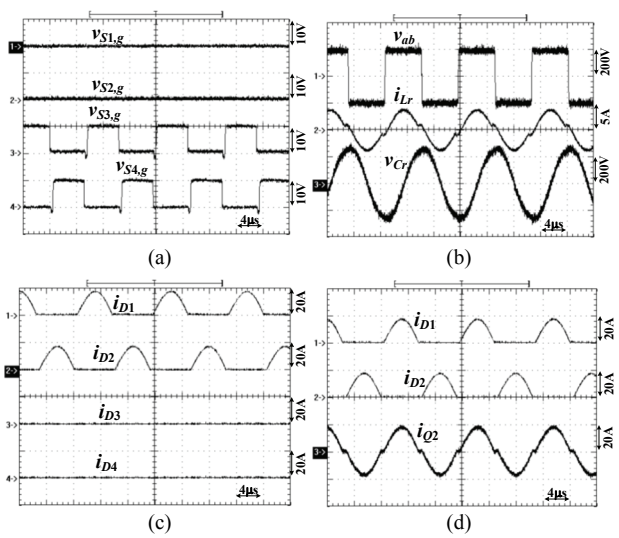

Fig. 9. Measured results at V_o=82V under the medium output voltage range. (a) Gating signals $v_{S1,g} \sim v_{S4,g}$ at a full load. (b) Primary side voltages and current v_{ab}, i_{Lr} and v_{Cr} at a full load. (c) Diode currents $i_{D1} \sim i_{D4}$ at a full load. (d) i_{D1}, i_{D2} and i_{Q2} at a full load.

strategy. Figs. 7 and 8 give measured results under low output voltage operation with V_o=40V and 78V, respectively. The gating voltages of S_1~S_4 for V_o=40V are shown in Fig. 7(a). It can be observed that S_1 and S_2 are off, and that S_3 and S_4 are turned on or off. The primary side voltages v_{ab} and v_{Cr}, the and current i_{Lr} at full load are given in Fig. 7(b) for V_o=40V. The output diode currents i_{D1}~i_{D4} are provided in Fig. 7(c) for V_o=40V. It is clear that all of the diodes are turned off under zero current switching. In the same manner, experimental waveforms of the proposed converter for V_o =78V at full load are illustrated in Fig. 8. Comparing the test results in Figs. 7 and 8, the switching frequency at V_o=40V is greater than the

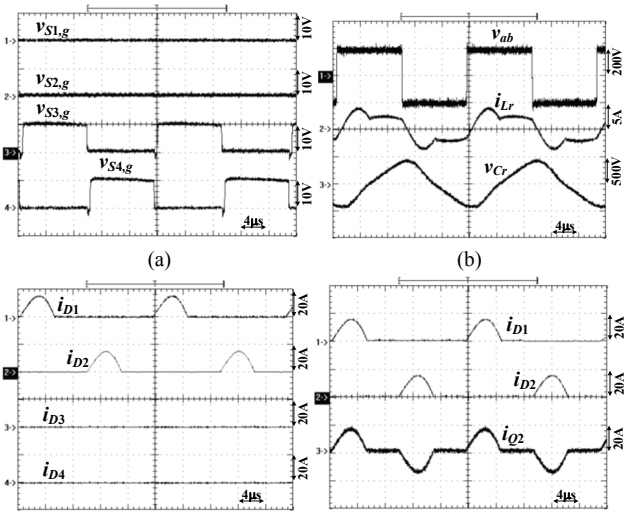

Fig. 10. Measured results at V_o=158V under the medium output voltage range. (a) Gating signals $v_{S1,g} \sim v_{S4,g}$ at a full load. (b) Primary side voltages and current v_{ab}, i_{Lr} and v_{Cr} at a full load. (c) Diode currents $i_{D1} \sim i_{D4}$ at full a load. (d) i_{D1}, i_{D2} and i_{Q2} at a full load.

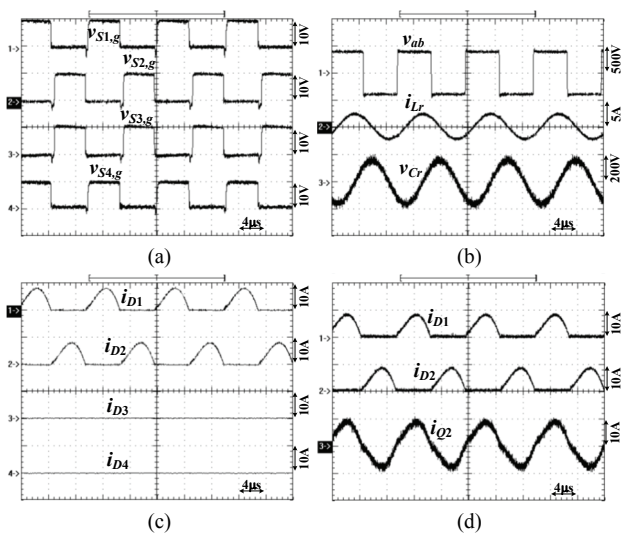

Fig. 11. Measured results at V_o=162V under the high output voltage range. (a) Gating signals $v_{S1,g} \sim v_{S4,g}$ at a full load. (b) Primary side voltages and current v_{ab}, i_{Lr} and v_{Cr} at a full load. (c) Diode currents $i_{D1} \sim i_{D4}$ at a full load; (d) i_{D1}, i_{D2} and i_{Q2} at a full load.

switching frequency at V_o=78V. For medium voltage range operation, S_1, S_2, D_3 and D_4 are off. Measured results at output voltages of V_o=82V and 158V are provided in Fig. 9 and 10, respectively. Figs. 9(a) and 9(b) provide experimental results of the gating voltages and primary waveforms at V_o=82V. The secondary side currents at V_o=82V are given in Figs. 9(c) and 9(d). Likewise, test results of the primary and secondary side waveforms for an 158V output voltage are demonstrated in Fig. 10. Comparing the test results in Figs. 9 and 10 for medium voltage operation, the converter operated

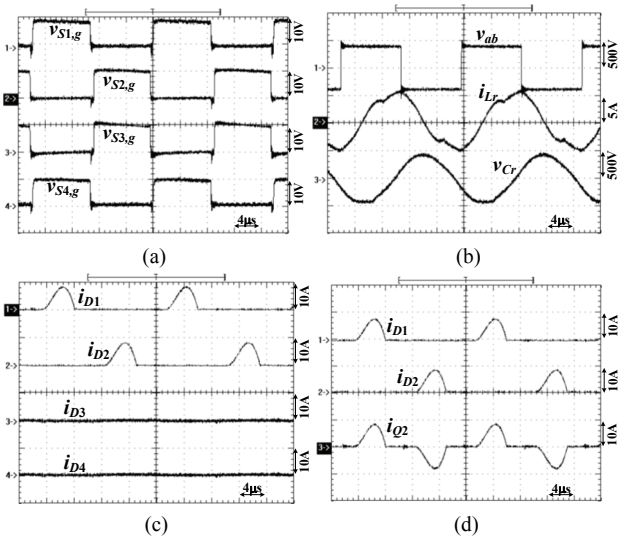

Fig. 12. Measured results at V_o=320V under the high output voltage range. (a) Gating signals $v_{S1,g}$ ~ $v_{S4,g}$ at a full load. (b) Primary side voltages and current v_{ab}, i_{Lr} and v_{Cr} at a full load. (c) Diode currents i_{D1} ~ i_{D4} at a full load. (d) i_{D1}, i_{D2} and i_{Q2} at a full load.

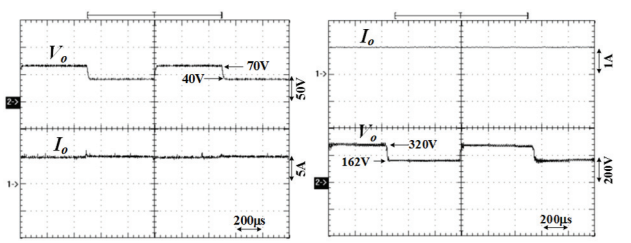

Fig. 13. Measured step response. (a) Between V_o=40V and 70V at I_o=5A. (b) Between V_o=162V and 320V at I_o=1A.

at an 82V output voltage has a higher switching frequency than in 158V output voltage case. For high voltage range operation, Q_1, D_3 and D_4 are off. The input side is a full-bridge series resonant circuit, and the output side is a half-bridge voltage-doubler rectifier. Fig. 11 gives test results under high output voltage operation and V_o=162V. Fig. 12 provides experimental results for V_o=320V and full load conditions. Measured converter efficiencies under a full load are 85.2%, 89.5%, 93.2% and 88.2% at V_o=40V, 82V, 162V and 360V, respectively. For a low voltage (high current) output, high conduction losses are observed on the secondary side. For the 360V output case, the converter has a low switching frequency and a high magnetizing current. Therefore, the primary *rms* current for V_o=320V is greater than the low output voltage case. Thus, larger conduction losses can be observed on the primary side for a V_o=320V output. Fig. 13(a) shows the step response between V_o=40V and 70V for the low output voltage range and I_o=5A. In the same manner, Fig. 13(b) provides the step response between V_o=162V and 320V for the high output voltage range and I_o=1A. No serious transient response is observed in the test results.

VI. CONCLUSIONS

This paper studies and implements a hybrid resonant converter with wide voltage range operation and low switching losses. To accomplish wide voltage range operation, two additional switches are adopted in a conventional full-bridge series resonant converter. One additional switch is used on the input side to achieve 4:1 output voltage range by the selection of a half-bridge or full-bridge series resonant converter. The other switch is adopted on the output side to realize a full-wave diode rectifier or voltage-doubler rectifier. Therefore, the output voltage range can be further extended to another 2:1 operation range. Since a series resonant converter is adopted in the proposed converter, both the active devices and passive diodes are operated under soft switching. Thus, the switching losses on the power semiconductors can be decreased. Two Schmitt voltage comparators are used in the control scheme to determine three output voltage ranges. There is a time delay when the output voltage is across different output voltage ranges. The theoretical circuit characteristics are confirmed by experiments conducted on a laboratory prototype. Future research will focus on improving the step response speed and avoiding unstable oscillations when the output voltage changes from the low output voltage range to the high output voltage range.

ACKNOWLEDGMENT

This research is supported by the Ministry of Science and Technology, Taiwan, under contract MOST 108-2221-E-224-022-MY2. The author would like to thank Mr. Ji-Wei Chang for his help to measure the circuit waveforms in the experiment.

REFERENCES

[1] G. Xu, D. Sha, Y. Xu, and X. Liao, "Dual-transformer-based DAB converter with wide zvs range for wide voltage conversion gain application," *IEEE Trans. Ind. Electron.*, Vol. 65, No. 4, pp. 3306-3316, Apr. 2018.

[2] H. Wu, Y. Li, and Y. Xing, "LLC resonant converter with semiactive variable-structure rectifier (SA-VSR) for wide output voltage range application," *IEEE Trans. Power Electron.*, Vol. 31, No. 5, pp. 3389-3394, May 2016.

[3] R. Beiranvand, M. R. Zolghadro, B. Rashidian, and S. M. H. Alavi, "Optimizing the LLC-LC resonant converter topology for wide-output-voltage and wide-output-load applications," *IEEE Trans. Power Electron.*, Vol. 26, No. 11, pp. 3192-3204, Nov. 2011.

[4] X. Wang, F. Tian, and I. Batarseh, "High efficiency parallel post regulator for wide range input DC–DC converter," *IEEE Trans. Power Electron.,* Vol. 23, No. 2, pp. 852-858, Mar. 2008.

[5] H. Wu, C. Wan, K. Sun, and Y. Xing, "A high step-down multiple output converter with wide input voltage range based on quasi two-stage architecture and dual-output *LLC* resonant converter," *IEEE Trans. Power Electron.,* Vol. 30, No. 4, pp. 1793-1796, Apr. 2015.

[6] C. Shang, L. Liu, M. Liu, and S. Men, "A highly-efficient two-stage DC-DC converter with wide input voltage," *Proc. IEEE INTELEC Conf.*, pp. 1-6, 2015.
[7] G. Zhou, X. Ruan, and X. Wang, "Input voltage feed-forward control strategy for cascaded DC/DC converters with wide input voltage range," *Proc. IEEE IPEMC Conf.*, pp. 603-608, 2016.
[8] Y. Jeong, J. K. Kim, J. B. Lee, and G. W. Moon, "An asymmetric half-bridge resonant converter having a reduced conduction loss for DC/DC power applications with a wide range of low input voltage," *IEEE Trans. Power Electron.,* Vol. 32, No. 10, pp. 7795-7804, Oct. 2017.
[9] P. Wang, L. Zhou, Y. Zhang, J. Li, and M. Sumner, "Input-parallel output-series DC-DC boost converter with a wide input voltage range, for fuel cell vehicles," *IEEE Trans. Veh. Tech.* Vol. 66, No. 9, pp. 7771-7781, Sep. 2017.
[10] Y. Zhang, C. Fu, M. Sumner, and P. Wang, "A wide input-voltage range quasi-Z-source boost DC-DC converter with high-voltage gain for fuel cell vehicles," *IEEE Trans. Ind. Electron.,* Vol. 65, No. 6, pp. 5201-5212, Jun. 2018.
[11] Z. Yao and J. Xu, "A three-phase DC-DC converter for low and wide input-voltage range application," *Proc. IEEE ITEC Conf.*, pp. 208-213, 2016.
[12] J. Lu, A. Kumar, and K.K. Afridi, "Step-down impedance control network resonant DC-DC converter utilizing an enhanced phase-shift control for wide-input-range operation," *IEEE Trans. Ind. Appl.,* Vol. 54, No. 5, pp. 4523-4536, Sep./Oct. 2018.
[13] H. Wu, C. Wan, K. Sun, and Y. Xing, "A high step-down multiple output converter with wide input voltage range based on quasi two-stage architecture and dual-output *LLC* resonant converter," *IEEE Trans. Power Electron.,* Vol. 30, No. 4, pp. 1793-1796, Apr. 2015.
[14] B. Kim, S. Kim, D. Y. Huh, J. H. Choi, and M. Kim, "Hybrid resonant half-bridge DC/DC converter with wide input voltage range," *Proc. IEEE APEC Conf.*, pp. 1876-1881, 2018.
[15] A.K. Singh, P. Das, and S.K. Panda, "Analysis and design of SQR-based high-voltage LLC resonant dc-dc converter," *IEEE Trans. Power Electron*., Vol. 32, No. 6, pp. 4466-4481, Jun. 2017.
[16] W. Sun, Y. Xing, H. Wu, and J. Ding, "Modified high-efficiency LLC converters with two split resonant branches for wide input-voltage range applications," *IEEE Trans. Power Electron.* Vol. 33, No. 9, pp. 7867-7870, Sep. 2018.
[17] M. M. Jovanović, and B. T. Irving, "On the fly topology-morphing control efficiency optimization method for LLC resonant converters operating in wide input and/or output-voltage range," *IEEE Trans. Power Electron.* Vol. 31, No. 3, pp. 2596-2608, Mar. 2016.

Bor-Ren Lin received his B.S. degree in Electronic Engineering from the National Taiwan University of Science and Technology, Taipei, Taiwan, in 1988; and his M.S. and Ph.D. degrees in Electrical Engineering from the University of Missouri, Columbia, MO, USA, in 1990 and 1993, respectively. From 1991 to 1993, he was a Research Assistant with the Power Electronic Research Center, University of Missouri. Since 1993, he has been with the Department of Electrical Engineering, National Yunlin University of Science and Technology, Yunlin, Taiwan, where he is presently a Distinguished Professor. His current research interests include power-factor correction, multilevel converters, active power filters, and soft-switching converters. Dr. Lin received a Fellowship position from the Institution of Engineering and Technology Association in 2017, and he is an Associate Editor of the *Institution of Engineering and Technology Proceedings—Power Electronics.* He was a recipient of Research Excellence Awards in 2004, 2005, 2007, 2011 and 2018 from the College of Engineering, National Yunlin University of Science and Technology. He received Best Paper Awards from the 2007 and 2011 IEEE Conference on Industrial Electronics and Applications, the 2007 Taiwan Power Electronics Conference, the 2009 IEEE–Power Electronics and Drive Systems Conference, the 2012 Taiwan Electric Power Engineering Conference, the 2014 IEEE–International Conference on Industrial Technology, and the 2019 IEEE–ICA SYMP Conference.